

Received 6 July 2022, accepted 3 August 2022, date of publication 16 August 2022, date of current version 23 August 2022.

Digital Object Identifier 10.1109/ACCESS.2022.3198943

APPLIED RESEARCH

Tuning Guidelines and Experimental Comparisons of Sine Based Auto-Tuning Methods for Fractional Order Controllers

ISABELA BIRS^{1,2,3}, CRISTINA MURESAN¹, MARCIAN MIHAI¹,
EVA DULF¹, (Senior Member, IEEE), AND ROBIN DE KEYSER^{2,3}

¹Department of Automation, Technical University of Cluj-Napoca, 400114 Cluj-Napoca, Romania

²DySC Research Group on Dynamical Systems and Control, Department of Electromechanical, Systems and Metal Engineering, Ghent University, 9052 Ghent, Belgium

³Flanders Make, EEDT—Decision and Control Group, 9052 Ghent, Belgium

Corresponding author: Cristina Muresan (cristina.muresan@aut.utcluj.ro)

This work was supported in part by the Romanian Ministry of Education and Research through CNCS-UEFISCDI within PNCDI III under Project PN-III-P1-1.1-TE-2019-0745 and Project PN-III-P1-1.1-PD-2021-0204 and in part by the Research Foundation Flanders (FWO) under Grant 1S04719N.

ABSTRACT Accurate process modeling is occasionally difficult. In such situations, auto-tuning methods enable the design of suitable controllers based on experimental data and predefined mathematical approaches. Fractional order PIDs have recently emerged as a generalization of the standard PID controller, but auto-tuning methods for these controllers are scarce. In this paper, three sine-test based methodologies are presented from a control engineer's perspective consisting of novel Sine-Test, FO-KC and FO-ZN methods, with clear design and implementation guidelines. The approaches are exemplified on a highly nonlinear experimental platform. An in depth comparison is performed based on experimental closed loop system performance for wide operating areas, tuning effort and complexity, with a focus on the suitability for industrial applications. The study aims at providing a solid foundation for practitioners that desire to explore auto-tuning possibilities, presenting tuning workflows and implementation guidelines, while also considering the challenges associated with real-life process.

INDEX TERMS Fractional order auto-tuners, auto-tuner comparison, nonlinear process, fractional calculus.

I. INTRODUCTION

It is without doubt that the PID controller is the king of industrial control. A recent analysis [1] published by Global Industry Analysts Inc., (GIA) states that the PID controller industry is bound to reach a whopping \$1.6 billion by 2026. Fresh perspectives on opportunities and challenges of a post-COVID industrial marketplace are explored in the report, for major end-use sectors such oil & gas, food & beverage, power, chemical, etc. Customer demands for high product quality, increasingly stringent safety regulations and intensified global competition lead to industrial processes operating under conditions that emphasize inherent nonlinearities. For large industrial plants, with highly coupled loop interactions, obtaining an accurate process model is strenuous

The associate editor coordinating the review of this manuscript and approving it for publication was Engang Tian¹.

work, justifying the usage of auto-tuning methods to obtain the controller's parameters [2], [3], [4].

Recent trends in controller auto-tuning enhance popular PID controllers with additional, fractional order differ-integral operators. Fractional order PID controllers are a generalization of the classical PID controller into the fractional calculus domain and was first introduced by I. Podlubny [5]. Numerous works prove the superiority of fractional order PID controllers in terms of improved closed loop system performance, increased stability and robustness with the addition of two parameters, consisting of arbitrary orders of integration and differentiation [6], [7], [8], [9]. Even if tuning methodologies of fractional order PID controllers are abundant [10], fractional order autotuning strategies are scarce featuring various limitations.

One of the first fractional order auto-tuners was introduced by [11], with controller design based on shaping

a 'flat-phase' around the gain crossover frequency leading to a controller similar to the classical PID, but with a fractional component s^λ . The relay test popular in integer order PID controller design is used in [7] to obtain a fractional order PI controller in series with a fractional order PD controller with a filter. The procedure uses specifications related to the gain crossover frequency, phase margin and robustness implying great effort in obtaining the controller's parameters.

The most popular auto-tuning methodology is Ziegler-Nichols, an easy approach that uses solely the process's critical gain associated to its critical frequency to determine integer order PID parameters. The method is known to perform poorly for reference tracking, but the disturbance rejection capabilities are good [2]. Several extensions of the ZN method aim at addressing the limitations of this methodology. In [12], the proportional and integral gains of the controller are computed using the popular Ziegler-Nichols (ZN) method, while an initial derivative gain is computed using Åström-Hägglund. A fine tuning method is employed to determine the optimal derivative gain by solving a system of two nonlinear equations built around a phase margin specification. The final tuning step is to determine the fractional orders of integration and differentiation with an optimization procedure. Again, the methodology is tedious and consists of a heavy, multi-step approach, with a major disadvantage in the optimization procedure which strongly depends on its initial values. Another study [13] extends the Ziegler-Nichols method in the fractional order domain, taking into consideration the time delay τ and an estimated process time constant T . A major limitation is that the methodology can be used only on systems that have an S-shaped step response. Other extensions of the ZN methodologies have been published in [30], [31], and [32], but all of them prove to be hard to apply to physical processes due to extensive tuning efforts and limitation such as the S-shaped response of the process.

Different approaches have been proposed by [18] through the *the Sine Test auto-tuner* and in [19] which introduces the *FO-KC auto-tuner*. In [18], the system is excited with a single sine test performed at the gain crossover frequency in order to measure the magnitude and phase of the output signal. Novel filtering techniques are used on the phase data to determine the phase slope. Nonlinear equations related to gain crossover frequency, phase margin and robustness through the isodamping property are solved using the experimentally acquired information. The FO-KC methodology introduced in [19] uses phase margin and isodamping frequency domain specifications to determine a forbidden region circle on the Nyquist diagram. A single sine test at the gain crossover frequency is further used to estimate the phase and phase slope of the process, as in the previously mentioned paper. The actual tuning procedure consists in minimizing the slope-difference between the loop frequency response and the forbidden region circle border, leading to an optimal fractional order PID controller.

A novel fractional order auto-tuner is proposed in [20], the *FO-ZN auto-tuner*. The method is based on a similar idea related to shaping the loop frequency response tangent to a defined Nyquist circle. The method is an extension to the Ziegler-Nichols approach based on a relay test that determined the process critical frequency and gain. The main benefit of the method is its ease of use, without needing any kind of optimization procedures to obtain fractional order PID controllers.

Currently, there are no studies available that compare fractional order auto-tuning methodologies. However, some works can be found such as [21] which compares 4 industrial integer order auto-tuners (ECA, Honeywell, τ -tuner and NOMAD) based on temperature experiments in a batch tank and a quadruple tank. In [22], an integer order KC controller is compared with SIMC, AMIGO and ZN ultimate gain auto-tuners for an experimental coupled tanks process. Again, only integer order methods are tackled. The abstract of [23] states that Ziegler-Nichols, Kappa-Tau, IMC-PID auto-tuning and data-based FRIT methods are compared with a fractional order auto-tuned PID controller. However, the paper is in Chinese and it is unclear what method was used to tune the fractional order PID controller.

The methods from [18], [19] have been successfully validated on multiple numerical examples. Since auto-tuners should be used in the absence of a process model, experimental validations are paramount in proving the importance of the proposed design strategies, especially for the case of nonlinear processes. The papers introducing these methods focus on theoretical contributions and mathematical proofs. Available experimental validations target a single process, lacking clear implementation strategies from the control engineer perspective. Currently, there are no experimental nor numerical validations available for [20], except transfer functions used in the original paper to validate the methodology.

The present study aims at offering a comparison between auto-tuning strategies, together with step by step guidelines on the practical design and implementation of the three methods from [18], [19], and [20] based on real-life challenges. The chosen system is a highly nonlinear experimental platform, exhibiting dynamics relevant for the mechanical field. All three works are different than the approaches usually encountered in auto-tuning literature, but similar among themselves through the usage of a single experimental sine test.

The novelty elements of the papers are: a ready to use auto-tuning and implementation guideline for real-life processes; comparisons between fractional order sine based strategies based on experimental results, respecting the general scope of auto-tuners; analysis on system performance, controller tuning effort and total duration of the necessary experiments. Furthermore, this work presents the first experimental assessment of the auto-tuner from [20].

The paper is structured as follows: Section II briefly presents the tuning strategies, summarizing essential information that needs to be taken into consideration in the tuning

procedure; Section III describes the experimental platform with a nonlinear analysis, followed by step-by-step auto-tuning procedures based exclusively on experimental data, real-life challenges of tuning and implementing fractional order controllers and possibilities to overcome them, while Section IV compares the three methodologies from the closed loop system's perspective as well as tuning difficulty. Finally, Section V concludes the paper.

II. SINE BASED AUTO-TUNERS - A CONTROL ENGINEER'S OVERVIEW

Starting with an integer order PID controller given by

$$C_{PID} = k_p \left(1 + \frac{1}{T_i s} + T_d s \right) \quad (1)$$

and generalizing it into the fractional order domain gives

$$C_{FOPID} = k_p \left(1 + k_i \frac{1}{s^\lambda} + k_d s^\mu \right), \quad (2)$$

where k_p , k_i , k_d are proportional gains, T_i and T_d are the integral and derivative time constants, and λ , μ are the fractional orders of integration and differentiation, respectively.

The most popular tuning methodology for fractional order controllers is based on imposing phase margin specifications related to gain crossover frequency ω_{gc} , phase margin φ_m and robustness [10], [24], [25], [26], [27]. The latter is defined based on a property known as *isodamping*, where a flat phase is imposed around the gain crossover frequency. This ensures that the system offers a certain degree of robustness for gain variations. The resulting system of nonlinear equations that give the parameters of a fractional order controller is

$$\angle(C(j\omega_{gc})P(j\omega_{gc})) = -\pi + \varphi_m, \quad (3)$$

$$|C(j\omega_{gc})P(j\omega_{gc})| = 1, \quad (4)$$

$$\left. \frac{d(\angle(C(j\omega)P(j\omega)))}{d\omega} \right|_{\omega=\omega_{gc}} = 0. \quad (5)$$

A. THE SINE TEST AUTO-TUNER

The method was initially introduced in [18]. The only experimental validation available for the sine test auto-tuner is presented in [28], where a fractional order PD controller is computed for suppressing unwanted vibrations in a smart-beam platform.

The base idea is to excite the process P with a sine wave of amplitude A_i and the desired gain crossover frequency (ω_{gc}), denoted by $u(t) = A_i \sin(\omega_{gc} t)$. The generated output, y , is a sine wave, with a different output amplitude A_o , the same ω_{gc} frequency and a time shift $\tau = t_i - t_o$. The magnitude M and phase φ are given by

$$M = |P(j\omega_{gc})| = \frac{A_o}{A_i}, \quad (6)$$

$$\varphi = \angle P(j\omega_{gc}) = \omega_{gc} \tau = \omega_{gc}(t_i - t_o). \quad (7)$$

Note that t denotes the time and $j = \sqrt{-1}$.

The novelty of this method lies in determining the phase derivative because there is no trivial, straightforward procedure for doing it. The idea is to pass the output through a second order filter to obtain another signal:

the output of the process derivative, followed by the phase slope. Assuming an input signal is $v(t) = tu(t)$ leading to an output $x(t)$, the following holds in the Laplace, s , domain:

$$\mathcal{L}\{tu(t)\}P(s) = X(s), \quad (8)$$

leading to

$$-\frac{dU(s)}{ds}P(s) = X(s). \quad (9)$$

If the initial input signal is applied to the derivative of the process, the output \bar{y} is given by

$$\frac{dP(s)}{ds}U(s) = \bar{Y}(s). \quad (10)$$

The derivative of the output signal is

$$\begin{aligned} \frac{dY(s)}{ds} &= \mathcal{L}\{-ty(t)\} \implies \\ \mathcal{L}^{-1} \left\{ \frac{dY(s)}{ds} \right\} &= \mathcal{L}^{-1} \left\{ \frac{d(P(s)U(s))}{ds} \right\}. \end{aligned} \quad (11)$$

The equation can be rewritten as

$$\frac{d(P(s)U(s))}{ds} = \bar{Y}(s) - X(s), \quad (12)$$

giving

$$-ty(t) = \mathcal{L}^{-1}\{\bar{Y}(s) - X(s)\}. \quad (13)$$

A sinusoidal input signal has the Laplace transform

$$U(s) = \frac{A_i \omega_{gc}}{s^2 + \omega_{gc}^2} \quad (14)$$

with its derivative

$$\frac{dU(s)}{ds} = -\frac{2A_i \omega_{gc} s}{(s^2 + \omega_{gc}^2)^2}, \quad (15)$$

leading to

$$\begin{aligned} X(s) &= -\frac{dU(s)}{ds}P(s) = -\frac{2A_i \omega_{gc} s}{(s^2 + \omega_{gc}^2)^2}P(s) \\ &= \frac{A_i \omega_{gc}}{s^2 + \omega_{gc}^2} \frac{2s}{s^2 + \omega_{gc}^2} P(s). \end{aligned} \quad (16)$$

Equation (14) and knowing that $U(s)P(s) = Y(s)$ give $X(s)$ as

$$X(s) = \frac{2s}{s^2 + \omega_{gc}^2} Y(s), \quad (17)$$

meaning that $x(t)$ can be computed by adding a second order filter, from where the process derivative $\bar{y}(t)$ can be computed as the difference between $x(t)$ and $ty(t)$. The testing procedure is depicted in Fig. 1.

The terms seen in the bottom of Fig. 1 are the complex representations of the signals $y(t)$ and $\bar{y}(t)$

$$\bar{M} = \frac{A_{\bar{y}}}{A_i} \quad (18)$$

$$\bar{\varphi} = \omega_{gc} \tau_{\bar{y}} = \omega_{gc}(t_i - t_{\bar{y}}) \quad (19)$$

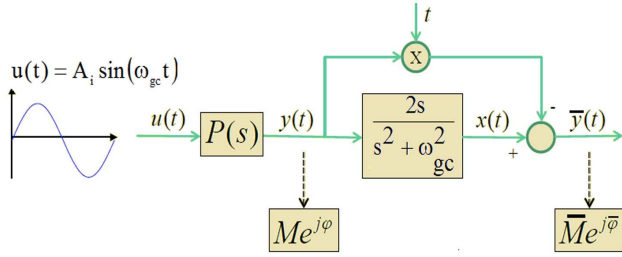


FIGURE 1. Experimental block scheme for the sine wave auto-tuner.

and the phase slope at gain crossover frequency is computed as

$$\frac{d \angle P(j\omega)}{j\omega} \Big|_{\omega=\omega_{gc}} = \frac{d\phi}{d\omega} \Big|_{\omega=\omega_{gc}} = \frac{\bar{M}}{M} \cos(\bar{\varphi} - \varphi). \quad (20)$$

a: CONTROL ENGINEER’S GUIDELINES

The following steps should be followed in the tuning procedure:

- 1) Establish the desired gain crossover frequency ω_{gc} and phase margin φ_m based on the desired values for the closed loop system’s settling time and overshoot
- 2) Excite the process with a sine test and register the input and output signals, $u(t)$ and $y(t)$
- 3) Compute $\bar{y}(t)$ using (17). The filter can be implemented in real-time directly on the process, or the registered signals at Step 2 can be used in an environment such as Simulink to generate the phase derivative.
- 4) Extract the modulus, phase and phase derivative of the process using (6), (7), (18), (19) and (20).
- 5) Solve the system of nonlinear equations comprised by (3), (4), (5) to determine the parameters of the controller.

b: TUNING NOTES

Base the choice of ω_{gc} and φ_m on realistic expectations of the controlled process. The frequency should be chosen with respect to the type of controller and the critical frequency of the process (e.g. if the tuned controller is a fractional order PI which introduces a negative phase and the chosen frequency is equal to the critical frequency, the closed loop system will be unstable). If the experimental system allows, the input sine wave should have an amplitude of 1 for simplicity of computations ($A_i = 1$). If the output signal is too noisy, an alternative to filtering is the usage of a pure sine signal (with the same properties) to compute the phase derivative. When solving the system of nonlinear equations at Step 5, a graphical approach is a straightforward and easy to implement solution, as opposed to complex mathematical strategies. Always check that the obtained controller has physical relevance (fractional orders belong in the (0 2) interval and proportional gains are greater than 0 [29]).

B. THE FO-KC AUTO-TUNER

The methodology was firstly introduced in [19], with some validations published in [30], [31], and [32] for a hemody-

namic cardiac output process, a robotic arm manipulator and a dynamical transfer function, respectively. The controller tuning has been performed on mathematical models of the process, not on experimental data, defying the general purpose of an auto-tuning method.

The strategy resembles the previous method by using the same data related to the process: the modulus, the phase and the derivative of the phase. The novelty of this approach lies in defining a ‘forbidden region’ circle on the Nyquist diagram. This region is based upon the gain and phase margins which are related to the performance specifications that the closed loop should achieve. The controller parameters should be computed such that the open loop touches the forbidden region’s border.

The main idea is described by Fig. 2, by moving a point B from the process’s Nyquist plot to a new point A with the help of the controller. The loop frequency response, denoted by $L(j\omega) = P(j\omega)C(j\omega)$, should be tangent to the forbidden region circle, meaning that the slope of the tangent is equal to the slope of $L(j\omega)$. Point D is obtained with respect to an imposed gain margin (GM), while E is based on the phase margin (PM). Trigonometric equations inside the circle give the forbidden region center C and radius R as

$$C = \frac{GM^2 - 1}{2GM(GM \cos PM - 1)} \quad R = C - \frac{1}{GM}, \quad (21)$$

which gives the slope of the forbidden region tangent in point A with respect to the angle α

$$\frac{d \operatorname{Im}}{d \operatorname{Re}} \Big|_{\alpha} = \frac{-R \sin \alpha + C}{R \cos \alpha} = \frac{\cos \alpha}{\sin \alpha}. \quad (22)$$

The slope of $L(j\omega)$ can be computed with respect to the derivative

$$\begin{aligned} \frac{dL(j\omega)}{d\omega} &= P(j\omega) \frac{dC(j\omega)}{d\omega} + C(j\omega) \frac{dP(j\omega)}{d\omega} \\ &= \frac{d \operatorname{Re}_{PC}}{d\omega} + j \frac{d \operatorname{Im}_{PC}}{d\omega} \end{aligned} \quad (23)$$

Equation (23) allows the computation of $\frac{d \operatorname{Im}_{PC}}{d\omega} \Big|_{\omega=\bar{\omega}}$, where $\bar{\omega}$ is the chosen test frequency. The following equation holds for point A

$$M_A e^{j\varphi_A} = M_{PC}(j\bar{\omega}) e^{j\varphi_{PC}(j\bar{\omega})} \quad (24)$$

which can be rewritten as

$$M_A = M_{PC}(j\bar{\omega}) = M_P(j\bar{\omega}) M_C(j\bar{\omega}), \quad (25)$$

$$\varphi_a = \varphi_{PC}(j\bar{\omega}) = \varphi_P(j\bar{\omega}) + \varphi_C(j\bar{\omega}). \quad (26)$$

The modulus and phase can also be computed trigonometrically as

$$\begin{aligned} M_A &= \sqrt{C^2 + R^2 - 2CR \cos \alpha} \\ \tan(\varphi_C + \varphi_P) &= \frac{R \sin \alpha}{C - R \cos \alpha} = \frac{\tan \varphi_C + \tan \varphi_P}{1 - \tan \varphi_C \tan \varphi_P} \\ \Rightarrow \tan \varphi_C &= \frac{R \sin \alpha - \tan \varphi_P (C - R \cos \alpha)}{\tan \varphi_P R \sin \alpha + (C - R \cos \alpha)} \end{aligned} \quad (27)$$

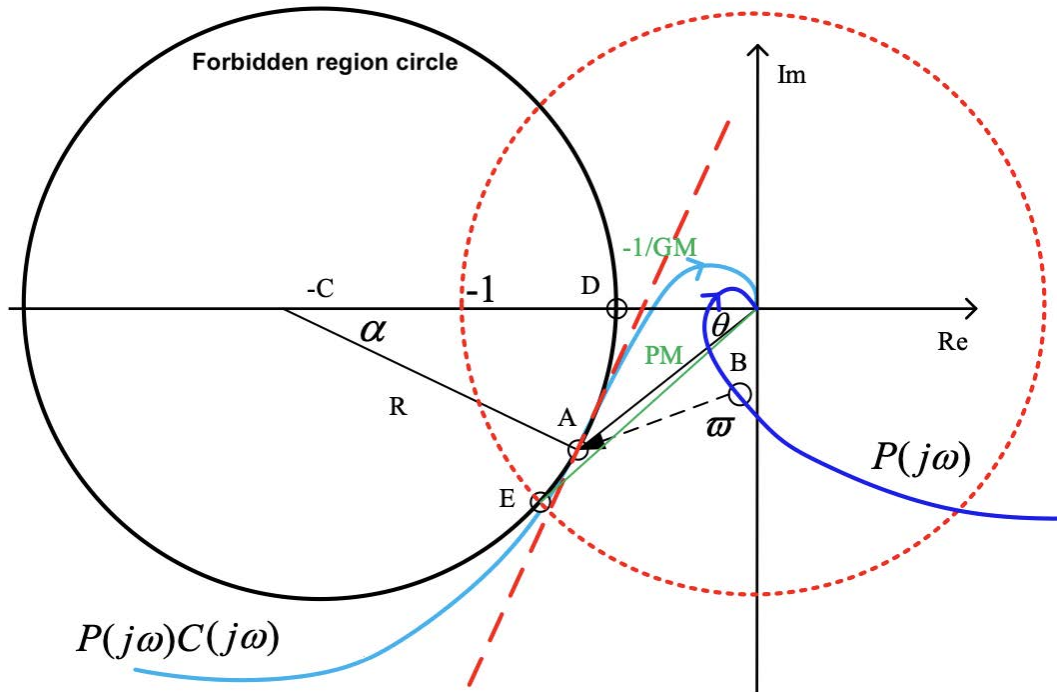


FIGURE 2. Tuning principle for the KC auto-tuner.

$P(j\bar{\omega})$, $\varphi_P(j\bar{\omega})$ and $\frac{dP(j\omega)}{d\omega}$ are computed according to [18] resulting in $\frac{d \text{Im}_{PC}}{d \text{Re}_{PC}} \Big|_{\omega=\bar{\omega}}$. The design translates into a minimization problem

$$\min_{\alpha} \left\| \frac{d \text{Im}}{d \text{Re}} \Big|_{\alpha} - \frac{d \text{Im}_{PC}}{d \text{Re}_{PC}} \Big|_{\omega=\bar{\omega}} \right\|, 0 \leq \alpha \leq 90^\circ. \quad (28)$$

a: CONTROL ENGINEER’S GUIDELINES

The following steps should be followed for the FO-KC auto-tuning procedure:

- 1) Select gain margin GM and phase margin PM values to ensure the stability of the closed loop system and desired performance.
- 2) Compute the forbidden region circle and α using (21).
- 3) Determine the slope of the forbidden region circle using (22).
- 4) Select the frequency $\bar{\omega}$ and perform an experimental sine tests on the process.
- 5) Compute the frequency response of $L(j\bar{\omega})$.
- 6) Taking points on the circle’s border in small increments, compute the desired fractional order controller.
- 7) Search for the point where the loop frequency response is tangent to the forbidden region circle using (28).
- 8) Determine the controller that corresponds to the point found at Step 7.

b: TUNING NOTES

The methodology has been validated for PM=45° and GM=2. It is a good idea to choose these values, especially for PM, in order to work with a right triangle which considerably

reduces computational effort. The FO-KC method should work for any $\bar{\omega}$, however all available validations use the critical frequency for the sine tests. The minimization problem can be solved with a simple *for* loop, by taking alpha in 1° increments and saving the best solution.

C. THE FO-ZN AUTO-TUNER

This is a novel auto-tuning strategy recently introduced by [20]. There are no validations available, except for the transfer functions used in the original paper to prove the veracity of the proposed approach. The main idea of this auto-tuner is to improve the standard fractional order Ziegler-Nichols control strategy, by shaping the “direction” of the loop frequency response in a chosen point on the Nyquist diagram. The method is similar to FO-KC auto-tuner previously presented through the usage of loop shaping in the Nyquist plot.

Exciting the system with a sinusoidal signal with amplitude A_i and the critical frequency ω_c generates an output signal with amplitude A_o and time period T_c . According to the classical ZN method, the integer order PID controller’s parameters from (1) are

$$k_p = 0.6 \frac{A_i}{A_o}, \quad T_i = \frac{T_c}{2}, \quad T_d = \frac{T_c}{8}. \quad (29)$$

The following relations related to the magnitude and phase of the process hold

$$\omega_c = \frac{2\pi}{T_c},$$

$$M = |P(j\omega_c)| = \frac{A_o}{A_i},$$

$$\begin{aligned} \varphi &= \angle P(j\omega_c) = -180^\circ, \\ P(j\omega_c) &= -\frac{A_o}{A_i}. \end{aligned} \quad (30)$$

Choosing the exact values from (29) and equating them with the PID controller transfer function from (1) in the frequency domain ($s = j\omega$) gives

$$\begin{aligned} C_{PID}(s) &= k_p \left(1 + \frac{1}{T_i j\omega_c} + T_d j\omega_c \right) \\ &= k_c (0.6 + 0.28j) \end{aligned} \quad (31)$$

leading to the loop frequency response

$$L_{PID}(j\omega_c) = -0.6 - 0.28j. \quad (32)$$

This results provides a stable working point that ensures acceptable performance for the closed loop system such as high overshoot (not desirable, but tolerable), reduced settling time (highly desirable). A better insight is presented in Fig. 3.

Fig. 3b shows a process that is too close of the -1 point, leading to less robustness, decreased stability and bad closed loop system performance. The FO-ZN auto-tuner aims at reshaping the response while keeping the operating point. In addition, the fractional order of differentiation and integration are considered equal. Rewriting the fractional order PID controller from (2) in the frequency domain in order to keep the notations used in the ZN methodology gives

$$C_{FOPID}(s) = k_p \left(1 + \frac{1}{T_i s^\mu} + T_d s^\mu \right). \quad (33)$$

In the FO-ZN methodology, T_d and T_i lose their meaning as time constants, with the real time constants being τ_i and τ_d

$$T_d = \tau_d^\mu, \quad T_i = \tau_i^\mu = r^\mu \tau_d, \text{ where } r = \frac{\tau_i}{\tau_d}. \quad (34)$$

The frequency domain specification of the controller becomes

$$C_{FOPID}(j\omega) = k_p \left(1 + \frac{1}{T_i (j\omega)^\mu} + \frac{T_i}{r^\mu} (j\omega)^\mu \right). \quad (35)$$

The following notations are introduced

$$\begin{aligned} R &= r^\mu, \\ (\pm j)^\mu &= \cos\left(\mu \frac{\pi}{2}\right) \pm j \sin\left(\frac{\pi}{2}\right) = C \pm jS, \\ X &= T_i \omega^\mu. \end{aligned} \quad (36)$$

Rewriting (35) with respect to (36) gives

$$\begin{aligned} C_{FOPID}(j\omega) &= k_p \left(1 + C \left(\frac{X}{R} + \frac{1}{X} \right) \right) \\ &\quad \cdot \left(1 + j \frac{S \left(\frac{X}{R} - \frac{1}{X} \right)}{1 + C \left(\frac{X}{R + \frac{1}{X}} \right)} \right) \\ &= a \left(1 + j \frac{b}{a} \right), \end{aligned} \quad (37)$$

leading to the following quadratic equation

$$\left(\frac{b}{a} C - S \right) X^2 + \left(\frac{b}{a} R \right) X + R \left(\frac{b}{a} C + S \right) = 0. \quad (38)$$

The quadratic equation above can be solved for any frequency ω , with the constraint $X > 0$.

The particular case of the ZN auto-tuner from (29) gives $a = 0.6 \frac{A_o}{A_i}$ and $\frac{b}{a} = 0.467$. Consequently, the following relations are obtained

$$\begin{aligned} k_p \left(1 + C \left(\frac{X}{R} + \frac{1}{X} \right) \right) &= 0.6 \frac{A_o}{A_i} \\ \implies k_p &= \alpha \frac{A_o}{A_i}, \alpha = \frac{0.6}{1 + C \left(\frac{X}{R} + \frac{1}{X} \right)} \\ X &= T_i \omega_c^\mu = T_i \left(\frac{2\pi}{T_c} \right)^\mu \\ \implies T_i &= \beta T_c^\mu, \beta = \frac{X}{(2\pi)^\mu} \\ T_d &= \frac{T_i}{R} \implies T_d = \gamma T_i, \gamma = \frac{1}{R} \end{aligned} \quad (39)$$

The existence condition related to the phase of the controller with respect to ZN is $\varphi = \text{atan}(0.28/0.6) = 25^\circ$. This means that the fractional order PID controller should produce a phase advance of 25° , with a maximum value known for this type of controller as 90° , giving $\mu_{min} = 0.28$.

a: CONTROL ENGINEER'S GUIDELINES

The FO-ZN auto-tuning method can be applied through the following steps:

- 1) Run multiple sinusoidal tests to determine the critical frequency of the process.
- 2) Compute the critical gain A_i/A_o and the critical time period T_c .
- 3) Compute α, β, γ using (39).
- 4) Select the value of r from (36) and $\mu > \mu_{min}$.
- 5) Compute the values of C, S and R according on (36).
- 6) Impose the ZN loop frequency response from (32) and compute the parameters a and b from (37).
- 7) Determine X by solving (38).
- 8) Compute α, β, γ from (39).
- 9) Finally, the controller's parameters k_p, T_i and T_d can be computed as shown in (39).

b: TUNING NOTES

One can select $r = 4$ at Step 4, corresponding to the ZN example. In this case, the quadratic equation from (37) becomes $(0.467C - S)X^2 + 0.467RX + R(0.467C + S) = 0$ where $X > 0$ is the desired solution. The phase advance produced by the fractional order PID controller with $\lambda = \mu$ is $\mu 90^\circ$. Base the choice of μ from step 3 on the desired phase advance for the selected r , keeping in mind that $\mu \geq 0.28$.

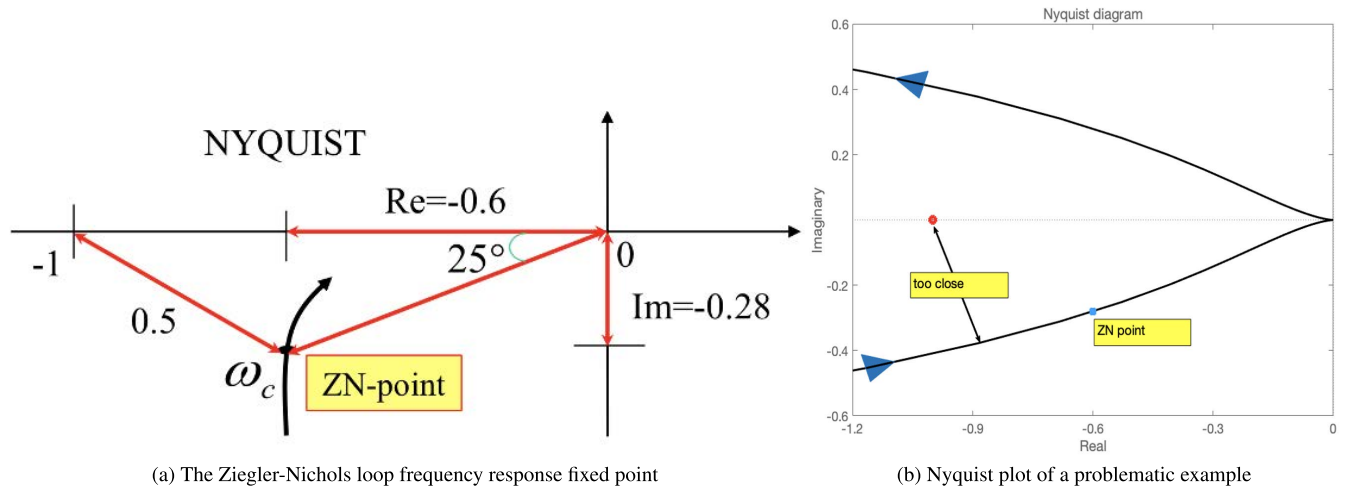


FIGURE 3. Nyquist analysis of the ZN method.

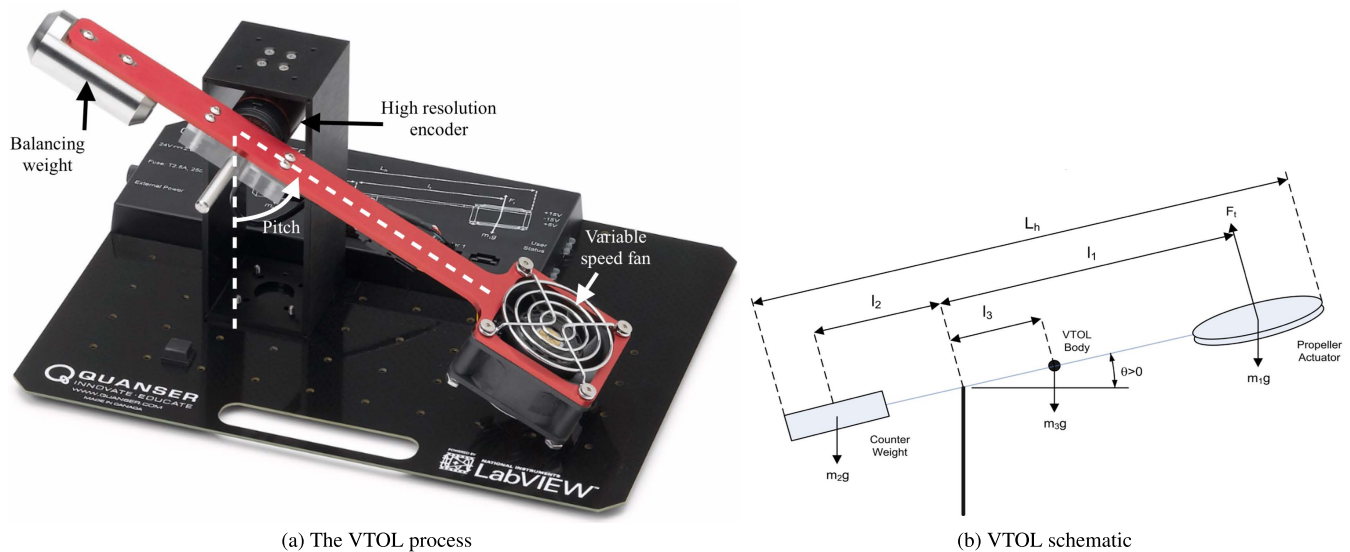


FIGURE 4. Experimental tests on the VTOL unit.

III. WORKING EXAMPLE

A. THE EXPERIMENTAL UNIT

The auto-tuners presented in Section II will be tested on a Vertical Take-Off and Landing (VTOL) Platform from Quanser. Fig. 4a shows a snapshot of the experimental setup, while Fig. 4b presents a block diagram of the rotating beam.

The moving arm (in Fig. 4a with red) is equipped with a balancing weight to the left and a variable speed fan to the right. Feeding the ventilator with a voltage between [0 10]V leads to the movement of arm, around a fixed point that is placed at 1/3 from its total length. The output signal is the angular position of the beam, measured by a high resolution encoder as the angle between a vertical line and the moving arm. Output values span in the $[-26\ 60]^\circ$ interval, with the 0° value corresponding to the horizontal position of the beam.

The process is highly nonlinear due to its construction, as shown in Fig. 4b. Experimental tests show that

the 0° position is obtained by applying 6.3V to the input. Fig. 5a shows the response of the VTOL unit to step inputs, exhibiting its nonlinear behavior. Fig. 5b presents the response of the experimental unit when excited with a sine wave of amplitude 1V and critical frequency 2.54rad/s (equivalent to 0.4Hz), with an amplitude of 6.3V. First, the platform reaches the horizontal position, followed at three identical sinusoidal inputs starting at $t = 14$ s.

The VTOL platform is connected to the NIElvis real-time data acquisition and control board from National Instruments. The data processing and controller implementation is done using LabVIEW, a graphical programming language.

The goal of the controller is to guide the moving arm at its reference position with minimum overshoot, reduced settling time, zero steady state position error, while also offering robustness. Since the platform is highly nonlinear, obtaining an accurate process model is difficult for a large operating

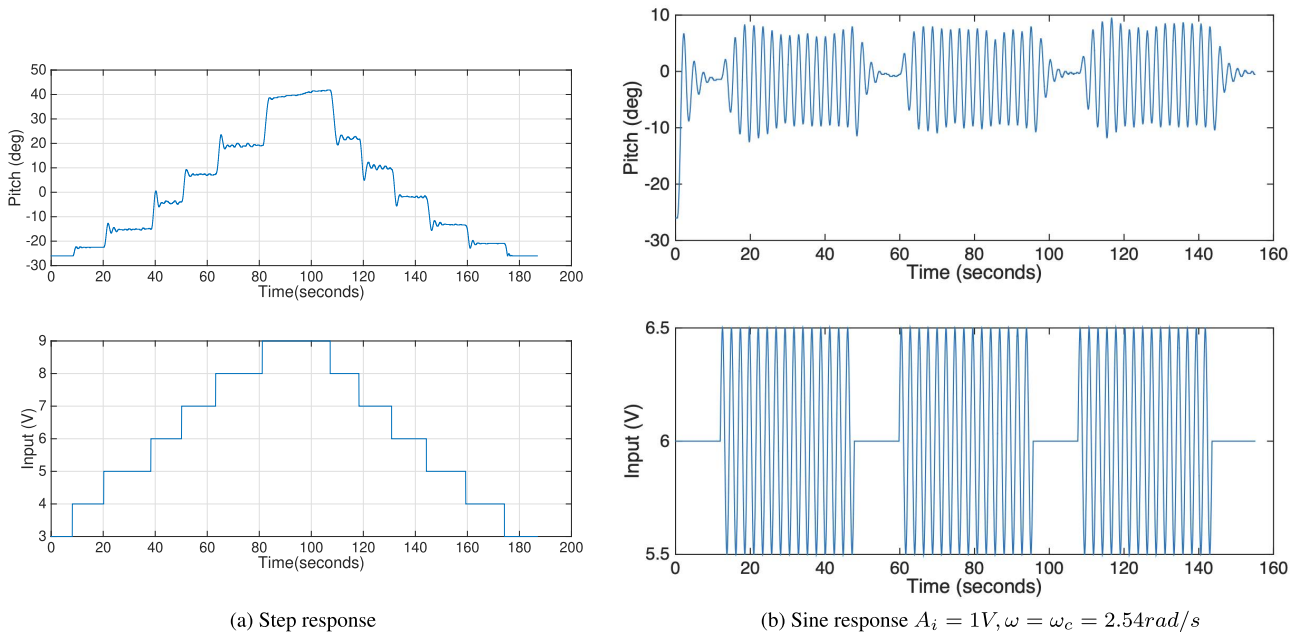


FIGURE 5. The experimental unit.

area, making fractional order auto-tuners ideal for determining the controller’s parameters in the absence of a mathematical model. The zero steady state position error design specifications justifies the usage of an integrator. Hence, only fractional order PI/PID controllers are suitable to control the system.

Determining a mathematical model for the VTOL system is not needed, since all the controllers are tuned using experimental data based on a sinusoidal input, without using a concrete mathematical representation of the system.

B. CONTROLLER AUTO-TUNING WITH THE SINE TEST METHOD

The VTOL critical frequency has been experimentally identified as 2.54rad/s. The system is marginally stable at the critical frequency, the phase is -180°, leading to the phase margin being 0°. A fractional order PI controller introduces a phase between $[-90\lambda\ 0]^\circ$. Therefore, ω_{gc} should be chosen considerably smaller than the critical frequency, compromising settling time for stability. The gain crossover frequency has been arbitrarily chosen as $\omega_{gc} = 0.1\ Hz = 0.62831\ rad/s$, with a phase margin that ensures the closed loop system’s stability $\varphi_m = 95^\circ$.

The next step implies applying the sine signal to the process and registering the output data. As shown in the previous subchapter, the VTOL process needs approx. 15 seconds to reach the 0° position. Hence, a step signal of amplitude 6.3V is applied for the first 15s, followed by a sine wave with amplitude $A_i = 1V$ and frequency $\omega_{gc} = 0.62831\ rad/s$. Fig. 6a shows the normalized input and output signals.

The process’s output is far from a perfect sine signal. Hence, the output sine wave is recreated and fed to the filter from (17). The generated output is the phase derivative \bar{y} ,

also shown in Fig. 6a. The environment used for this step is Matlab/Simulink. An alternative is computing the phase derivative directly in LabVIEW with a prior filtering performed real-time on the VTOL’s output. If the latter approach is chosen, one must ensure that the real-time denoiser doesn’t introduce delays in the signal that is fed to the second order filter.

The magnitude is obtained with respect to the input (A_i) and output (A_o) amplitudes of the signals as $M(j\omega_{gc}) = 10.757$. Furthermore, the phase $\varphi(j\omega_{gc}) = -15.5043^\circ$ is determined by multiplying the frequency with the time difference between two consecutive zero crossings of the input and output signals, respectively. The magnitude and phase of \bar{y} are $M(j\omega_{gc}) = 4.5764$ and $\varphi(j\omega_{gc}) = -3.1418\ rad$, leading to $\frac{d\angle P(j\omega)}{d\omega} \Big|_{\omega=\omega_{gc}} = -0.4099\ rad$.

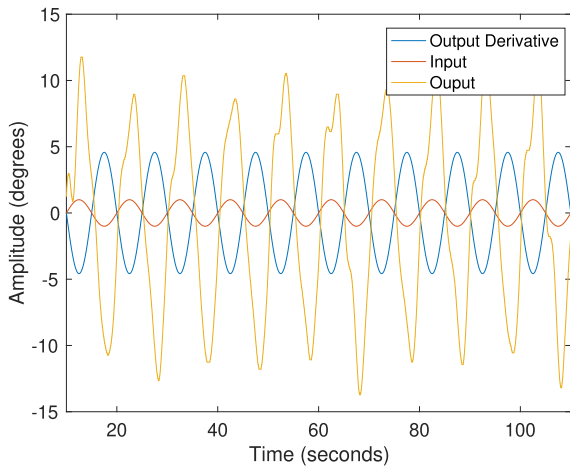
The last step is to solve the system of nonlinear equations (3)-(5) in order to obtain the parameters of a fractional order PI controller described by

$$C_{FOPI}(s) = k_p \left(1 + \frac{k_i}{s^\lambda} \right). \tag{40}$$

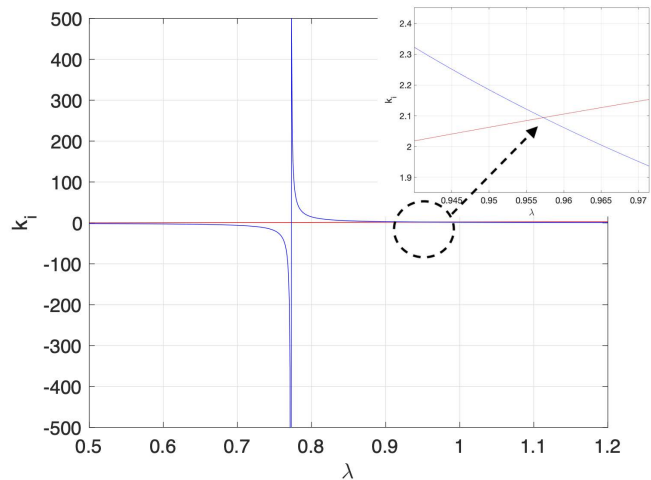
A simple graphical approach is employed, where λ is varied between (0 2) (based on existence conditions of fractional order controllers [29]). The integral gain k_i is computed based on the phase margin (4) and robustness (5) specifications for every λ . The result is shown in Fig. 6b. The value of $k_i = 2.0942$ is at the intersection of the plots, for $\lambda = 0.9572$. The proportional gain $k_p = 0.0267$ is obtained by replacing k_i and λ in the magnitude equation from (3).

Finally, the Sine Test controller is obtained as

$$C_{Sine-Test}(s) = 0.0267 \left(1 + \frac{2.0942}{s^{0.9572}} \right). \tag{41}$$



(a) Normalized input, output and output derivative signals



(b) Graphical solution for k_i

FIGURE 6. Controller tuning using the sine test auto-tuner.

C. CONTROLLER AUTO-TUNING WITH THE FO-KC METHOD

This subsection aims at tuning a fractional order PI controller with the transfer function expressed in (40). Choosing the same $\omega_{gc} = 0.1 \text{ Hz}$ and $\varphi_m = 95^\circ$ as for the Sine Test method is unsuitable for this auto-tuner, since the loop frequency response should intersect the forbidden region circle in the 3rd quadrant. Hence, the phase margin is limited between the (0 90) interval. The gain crossover frequency $\omega_{gc} = 0.185 \text{ Hz} = 1.1623 \text{ rad/s}$ (less than the critical frequency) and $\varphi_m = 80^\circ$ (realistic phase margin expectation based on the phase introduced by the fractional order PI controller) have been chosen for the FO-KC auto-tuning.

The next step is to compute the forbidden region circle $C = 5.7587$, $R = 5.6713$ and $\alpha = 10^\circ$. The tangent of the forbidden region circle in the working point is $\tan \alpha = 0.1763$.

The experimental platform is fed with a sinusoidal signal of amplitude 1V, frequency 0.185 Hz and offset 6.3V after the moving arm reaches 0°. The normalized input, output and phase derivative values are shown in Fig. 7. The phase derivative was computed using the same strategy as for the Sine Test auto-tuner.

The magnitude and phase are obtained as $M(j\omega_{gc} = 12.8413)$ and $\varphi(j\omega_{gc}) = -0.6376 \text{ rad}$. For the output derivative the following values are determined: $M(j\omega_{gc}) = 6.577$, $\bar{\varphi} = -3.1698 \text{ rad}$, leading to $\left. \frac{d\angle P(j\omega)}{j\omega} \right|_{\omega=\omega_{gc}} = -0.42 \text{ rad}$.

The last step is to solve the minimization problem from (28). Several approaches can be used for this, such as for loops and graphical approaches or directly using Matlab built-in functions such as *fmincon* from the System Optimization Toolbox.

The obtained FO-KC controller with the FO-KC method is

$$C_{FO-KC}(s) = 0.031 \left(1 + \frac{2.6048}{s^{0.9651}} \right). \quad (42)$$

Running the Sine Test auto-tuner for the chosen gain crossover frequency and phase margin gives a very similar controller to (41).

D. CONTROLLER AUTO-TUNING USING THE FO-ZN AUTO-TUNER

The last method involves performing a sine test with amplitude $A_i = 1 \text{ V}$ (for simplicity) and the critical frequency $\omega_c = 2.56 \text{ rad/s}$. The critical gain is identified as $K_c = A_i/A_o = 0.0692$, while the critical period is $T_c = 2.4546$. The input sine signal and the response of the VTOL are shown in Fig. 8. This method doesn't need the phase derivative, simplifying the data processing operations.

The integral and derivative time constants ratio is selected as $r = 4$ in order to keep the original ZN loop response. The study introducing the FO-ZN methodology suggests that the fractional order should be chosen based on the desired process response. However, since the other two methods gave a fractional order of integration of approx. 0.95, this value will be used further in order to perform a fair comparison. Hence, the fractional order of integration and differentiation is chosen as $\lambda = \mu = 0.95$.

The workflow of the mathematical computations is decided by the priority of the intermediate variables in (39). The following values are obtained: $b/a = 0.4667$, $C = 0785$, $S = 0.9969$, $R = 3.7321$, $X = 3.1006$, $\alpha = 0.5502$, $\beta = 0.5420$, and $\gamma = 0.2679$. The FO-ZN fractional order PID controller is

$$C_{FO-ZN}(s) = 0.0381 \left(1 + \frac{1}{1.272^{0.95}} + 0.3408^{0.95} \right). \quad (43)$$

IV. RESULTS, DISCUSSIONS, AND COMPARISONS

A. DISCRETE-TIME IMPLEMENTATION

The controllers from (41), (42) and (43) have been approximated in the discrete-time domain using the method from [33].

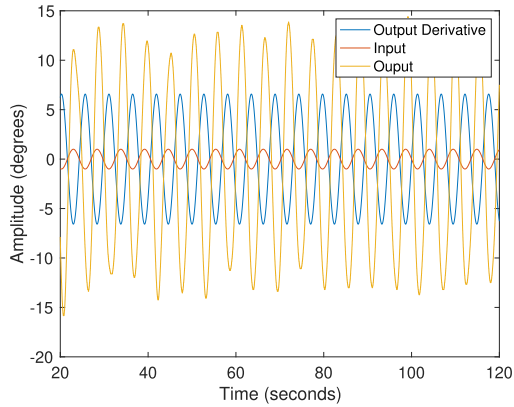


FIGURE 7. Normalized input and output signals for the FO-ZN auto-tuner.

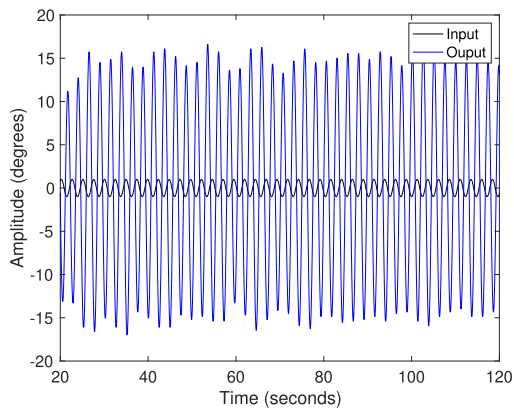


FIGURE 8. Normalized input and output signals for the FO-ZN auto-tuner.

A fifth order of approximation is used for every controller to determine the discrete-time recurrence formula, with a sampling time of 0.01s. Fig. 9 proves that the fifth order is suitable to accurately approximate the FO-ZN controller from (43) by comparing the frequency domain response of the fractional order controller with its approximation. As can be seen, the fifth order discrete-time transfer function has a similar frequency domain behaviour as the continuous-time fractional order controller. The results are similar for the Sine Test and FO-KC controllers.

The recurrence relations are used to compute the controller's parameters using LabVIEW and the value is fed to the experimental platform through the NIELvis microcontroller. The control signal is the voltage applied to the variable speed fan, limited in the [0 10]V interval due to the physical construction of the platform.

B. EXPERIMENTAL VALIDATION

The discrete-time controllers have been implemented in LabVIEW using their recurrence formulas, all having the same sampling time: 0.01s and the same complexion of 5th order. The controllers are validated based on three test scenarios related to reference tracking, disturbance rejection and robustness to system uncertainties.

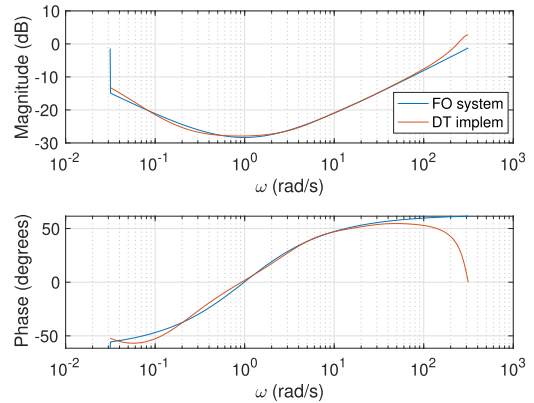


FIGURE 9. Frequency domain response of the fractional order PID controller (FO-ZN) with its discrete-time approximation.

a: REFERENCE TRACKING

Fig. 10 presents experimental test results for different operating areas. In Fig. 10a, the input steps are $[-20, -15, -20, -26]^{\circ}$. The -26° value represents the initial state of the VTOL system, where the moving arm lies on the base platform. As can be seen, all three controllers provide a closed loop system that is stable and reaches the desired set-point with zero steady state error. For the first test $[-26 -20]^{\circ}$, the FO-KC controller has a settling time of 20s, followed by the Sine-Test controller with 30s and the FO-ZN with a settling time of approx. 40s. However, for the other step values, the settling time is almost similar, with a slight improvement noticed for the FO-KC controller. Furthermore, the overshoot is null for all controllers. From the control signal point of view, the values vary between [0 4.8]V for the FO-KC and FO-ZN controllers, while the FO-ZN controller presents some spikes when the reference step amplitude changes. It is without doubt that the FO-KC controller is the best choice for this operating area.

A second step test is presented in Fig. 10b, where the set-point is $[0, 15, 30, 15]^{\circ}$. Again, the VTOL system is in its initial position at the beginning of the experiment, leaving from the -26° position. The FO-KC is the worst performer in this operating area, proving unstable. For the first two steps between $[-26 0]^{\circ}$, and $[0 15]^{\circ}$ the Sine-Test controller obtains the best settling time. However, for a wider operating area, the Sine-Test controller becomes unstable when the reference values go from 15° to 30° . The control signal is similar to the previous test case scenario, with several spikes observed on the control signal computed with the FO-ZN controller. Hitherto, the best controller for this test case is the FO-ZN, since it provides a stable closed loop system for all reference values.

b: DISTURBANCE REJECTION

Another test scenario implies output disturbance rejection performance presented in Fig. 11. The robotic arm is stabilized at -10° , between 0 and 35 seconds (best settling time is obtained with the FO-KC controller). An output disturbance

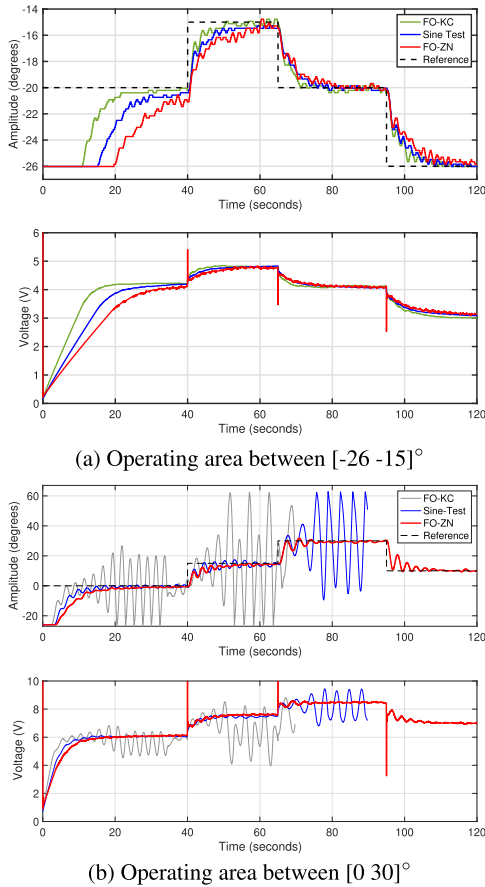


FIGURE 10. Experimental controller validation for step reference tracking.

of 7° is applied at $t=35s$. As can be seen, all three controllers successfully reject the disturbance. At $t=50s$, the disturbance is removed and the system returns to the reference position. The peak amplitude is larger for the FO-KC controller (-2°) which surpasses the disturbance amplitude, while the other controllers have a peak amplitude of -9° , less than the disturbance signal. Similar settling times are obtained by all three controllers. However, it can be observed that the FO-KC and Sine-Test controllers, cause larger output oscillations, while FO-ZN provides a smoother transition.

c: ROBUSTNESS

The last experiment targets robustness assessment for system uncertainties. Hence, the process is modified by adding a 20g weight to the moving arm on top of the fan. Another step reference test is performed for the $[-26 0]^\circ$ operating area, where all controllers proved stable in previous tests. Reference step values of $[-17, -10, 0]^\circ$ are applied at times $[0, 40, 65]s$. The FO-KC controller is considerably faster between $[-26 -17]^\circ$, followed by the Sine-Test controller and FO-ZN. For the $[-17 10]^\circ$ interval, all three controllers are similar, while for $[-10 0]^\circ$ the FO-KC controller is unstable. For the last interval, the controller tuned using the Sine-Test method provides a slight improvement to the settling time. It is clear that stability and improved settling time justifies the fact that the Sine-Test controller is the most robust.

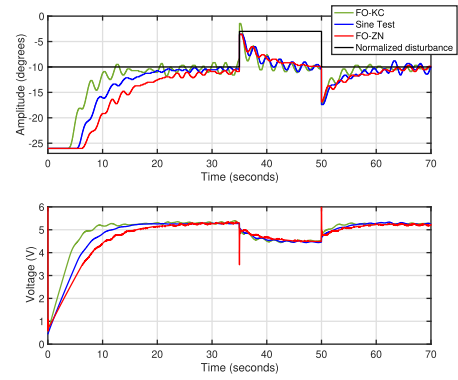


FIGURE 11. Experimental controller validation for output disturbance rejection.

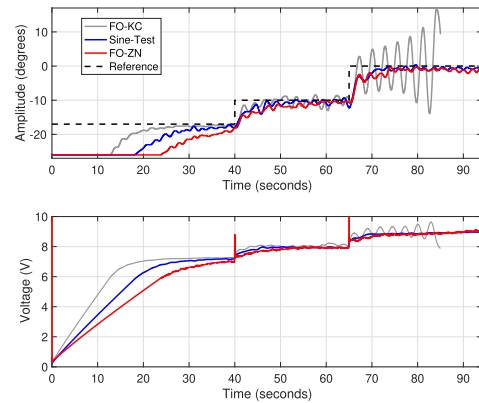


FIGURE 12. Experimental controller validation for system uncertainties.

C. CONTROLLER COMPARISON

The three tuning methodologies are compared based on the following criteria: closed loop system performance, tuning difficulty and tuning effort.

Table 1 presents a summary of the results presented in previous subsection related to closed loop system performance and control effort. The controllers receive a grade on a scale from 0 to 3, where 0 - poor, 1 - deficient, 2 - satisfactory and 3 - good.

For the $[-26 0]^\circ$ operating area the FO-KC controller outperforms the other controllers in terms of settling time. However, the FO-KC is graded with a 0 for step reference tracking in the $[0 30]^\circ$ range because it is unstable for all step amplitudes, while the Sine-Test controller is stable for 2 out of 3 step amplitudes. It is clear that the most reliable controller for nonlinear systems is the one tuned using the FO-ZN methodology. The control signal comparison is related to the aggressiveness of the controllers, where the FO-ZN receives a satisfactory grade due to spikes in the signal. These also need to be saturated before feeding the control signal to the real process. The implementation complexity is similar between the three compared controllers since all needed a fifth order discrete-time approximation for the same sampling time of 0.01s.

TABLE 1. Controller comparison based on closed loop system performance for the VTOL system.

| Criteria | Sine-Test | FO-KC | FO-ZN |
|-----------------------------------|-----------|-------|-------|
| <i>Performance</i> | | | |
| Step reference $[-26\ 0]^\circ$ | 2 | 3 | 2 |
| Step reference $[0\ 30]^\circ$ | 1 | 0 | 3 |
| Disturbance rejection | 2 | 2 | 3 |
| Robustness $[-26\ 0]^\circ$ | 3 | 0 | 2 |
| Robustness $[0\ 30]^\circ$ | 1 | 0 | 3 |
| Reliability for nonlinear systems | 2 | 1 | 3 |
| <i>Control signal</i> | | | |
| Aggressiveness | 3 | 3 | 2 |
| Saturation | 3 | 3 | 2 |
| Implementation complexity | 3 | 3 | 3 |

TABLE 2. Controller comparison based on tuning complexity.

| Criteria | Sine-Test | FO-KC | FO-ZN |
|-------------------------------------|-----------|----------|-------|
| <i>Prerequisites to auto-tuning</i> | | | |
| Critical frequency | x | x | x |
| Sine experiment | x | x | x |
| Output derivative | x | x | |
| Experimental data effort | Moderate | Moderate | Easy |
| <i>Tuning procedure</i> | | | |
| Nonlinear system solving | x | | |
| Optimization tasks | | x | |
| Specialized knowledge | x | x | |
| Computational effort | Moderate | Hard | Easy |

The conclusion of the performance comparison is that the FO-KC controller is the better choice for isolated operating ranges, while the FO-ZN controller is ideal for wider operating areas due to its increased stability in favor of settling time.

A different comparison is performed in Table 2 based on tuning complexity of the three methodologies. The presence of the specified criteria in the tuning procedure is marked with an 'x'. Finding the critical frequency is relevant for all three cases: in the FO-KC and Sine-Test methods, the gain crossover frequency is chosen to be less than the critical frequency in order to obtain a stable closed loop system, whereas the FO-ZN controller needs the sine test at the critical frequency. The sine test is also needed for every auto-tuning strategy. However, the Sine-Test and FO-KC methods needs an extra processing of the output signal, to obtain the output derivative signal. From the previously mentioned factors, the FO-ZN auto-tuner is an easier approach, since the output derivative is not needed.

In addition, another comparison is performed based on the road-map of the auto-tuning procedure. The Sine-Test auto-tuner requires the solving of a system of nonlinear equations, while the FO-KC auto-tuner implies minimizing the slope difference between the loop response and the forbidden region circle. However, instead of performing complex minimization procedures, it is sufficient to calculate the slope difference for 1° steps of the angle α and pick the one that gives the smallest difference. In comparison, the FO-ZN methodology implies choosing a fractional order (the same value for both integration and differentiation) and performing simple computations using predefined formulas. The most difficult task in the FO-ZN auto-tuning procedure is solving a trivial second order equation. Hence, the computational effort

is moderate for FO-KC and Sine-Test strategies and easy for the FO-ZN method.

Specialized knowledge in the field of calculus and optimization strategies is needed for the first two methods, whereas the FO-ZN is an easy and straightforward approach for anyone that doesn't have an engineering background. This makes the FO-ZN auto-tuner the better approach for industrial settings where robustness and stability are needed. However, the FO-KC methodology is ideal for applications with restricted operating areas where settling time is the most important design characteristic.

Comparing the tuning effort with the overall performance, the FO-ZN controller is definitely the better option because it obtains good performance with minimum effort and can be easily tuned without an extensive knowledge in the field of mathematics or control engineering.

V. CONCLUDING REMARKS

The paper presents three novel auto-tuning methodologies which are similar in using a single sine test for the tuning process. The method is suitable for stable processes. A brief mathematical background of fractional order PI/PID controllers is presented with the purpose of understating the tuning concepts. The methodologies are presented using a highly nonlinear VTOL platform, with the purpose of keeping a robotic arm at a given position, regardless of disturbance and process uncertainties. The tuning procedure is illustrated from a control engineer's perspective, with detailed explanations of the workflow, focusing on real-life data and implementation strategies. This work can be used as a general guideline when dealing with sine-based fractional order auto-tuners that can benefit both specialized engineers and non-specialized practitioners alike.

In addition, this work is the first comparison between fractional order auto-tuning strategies based on experimental data. Performance criteria, as well as tuning effort and complexity are analyzed in order to determine the best fractional order control strategy. The general conclusion of the study is that the FO-ZN controller is the most reliable and easy to tune option, whereas the FO-KC controller obtains the best performance for limited operating areas.

Future developments include, but are not limited to, testing the auto-tuning strategies on more mechanical processes and comparisons with other integer/non-integer methodologies.

REFERENCES

- [1] *PID Controllers—Global Market Trajectory and Analytics MCP13995*, Geological Institute of America, Carlsbad, CA, USA, 2021.
- [2] S. Hornsey, "A review of relay auto-tuning methods for the tuning of PID-type controllers," *Reinvention, Int. J. Undergraduate Res.*, vol. 5, no. 2, 2012. [Online]. Available: <https://www.warwick.ac.uk/reinventionjournal/archive/volume5issue2/hornsey>
- [3] C. Yu, "Autotuning of PID controllers," *Assem. Autom.*, vol. 20, no. 1, pp. 86–87, Mar. 2000.
- [4] M. Zhuang and D. P. Atherton, "Automatic tuning of optimum PID controllers," *IEE Proc. D (Control Theory Appl.)*, vol. 140, no. 3, p. 216, 1993.
- [5] I. Podlubny, "Fractional-order systems and $PI^{\lambda}D^{\mu}$ -controllers," *IEEE Trans. Autom. Control*, vol. 44, no. 1, pp. 208–214, Jan. 1999.
- [6] Y. Q. Chen, I. Petráš, and D. Xue, "Fractional order control—A tutorial," in *Proc. Amer. Control Conf.*, Jun. 2009, pp. 1397–1411.

- [7] C. A. Monje, B. M. Vinagre, V. Feliu, and Y. Chen, "Tuning and auto-tuning of fractional order controllers for industry applications," *Control Eng. Pract.*, vol. 16, no. 7, pp. 798–812, Jul. 2008.
- [8] S. Sondhi and Y. V. Hote, "Fractional order controller and its applications: A review," *Proc. AsiaMIC*, 2012, pp. 1–6.
- [9] Z. Wang, C. Wang, L. Ding, Z. Wang, and S. Liang, "Parameter identification of fractional-order time delay system based on legendre wavelet," *Mech. Syst. Signal Process.*, vol. 163, Jan. 2022, Art. no. 108141. [Online]. Available: <https://www.sciencedirect.com/science/article/pii/S0888327021005215>
- [10] I. Birs, C. Muresan, I. Nascu, and C. Ionescu, "A survey of recent advances in fractional order control for time delay systems," *IEEE Access*, vol. 7, pp. 30951–30965, 2019.
- [11] Y. Chen, K. Moore, B. Vinagre, and I. Podlubny, "Robust PID controller autotuning with a phase shaper," in *Proc. 1st IFAC Workshop Fractional Differentiation Appl.*, 2004, pp. 162–167.
- [12] C. Yeroglu, C. Onat, and N. Tan, "A new tuning method for $PI\lambda D\mu$ controller," 2009, pp. II–312.
- [13] D. Valerio and J. S. da Costa, "Tuning of fractional PID controllers with Ziegler–Nichols-type rules," *Signal Process.*, vol. 86, no. 10, pp. 2771–2784, 2006. [Online]. Available: <https://www.sciencedirect.com/science/article/pii/S0165168406000624>
- [14] M. Tajjudin, M. H. F. Rahiman, N. M. Arshad, and R. Adnan, "Robust fractional-order PI controller with Ziegler–Nichols rules," *Int. J. Elect. Comput. Eng.*, vol. 7, no. 7, pp. 1034–1041, 2013.
- [15] J. J. Gude and E. Kahoraho, "Modified Ziegler–Nichols method for fractional PI controllers," in *Proc. IEEE 15th Conf. Emerg. Technol. Factory Automat. (ETFA 2010)*, Sep. 2010, pp. 1–5.
- [16] A. Mughees and S. A. Mohsin, "Design and control of magnetic levitation system by optimizing fractional order PID controller using ant colony optimization algorithm," *IEEE Access*, vol. 8, pp. 116704–116723, 2020.
- [17] P. Chen, Y. Luo, Y. Peng, and Y. Q. Chen, "Optimal robust fractional order $PI^{\lambda}D$ controller synthesis for first order plus time delay systems," *ISA Trans.*, vol. 114, Aug. 2021, pp. 136–149.
- [18] R. De Keyser, C. I. Muresan, and C. M. Ionescu, "A novel auto-tuning method for fractional order PI/PD controllers," *ISA Trans.*, vol. 62, pp. 268–275, May 2016.
- [19] R. De Keyser, C. I. Muresan, and C. M. Ionescu, "Autotuning of a robust fractional order PID controller," *IFAC-PapersOnLine*, vol. 51, no. 25, pp. 466–471, 2018.
- [20] C. I. Muresan and R. De Keyser, "Revisiting Ziegler–Nichols. A fractional order approach," *ISA Trans.*, 2022. [Online]. Available: <https://www.sciencedirect.com/science/article/pii/S0019057822000234>, doi: 10.1016/j.isatra.2022.01.017.
- [21] J. Berner, K. Soltesz, T. Hägglund, and K. J. Åström, "An experimental comparison of PID autotuners," *Control Eng. Pract.*, vol. 73, pp. 124–133, Apr. 2018.
- [22] R. D. Keyser and C. I. Muresan, "Validation of the KC autotuning principle on a multi-tank pilot process," *IFAC-PapersOnLine*, vol. 52, no. 1, pp. 178–183, 2019. [Online]. Available: <https://www.sciencedirect.com/science/article/pii/S2405896319301429>
- [23] W. Zhang and M. Yang, "Comparison of auto-tuning methods of PID controllers based on models and closed-loop data," in *Proc. 33rd Chin. Control Conf.*, Jul. 2014, pp. 3661–3667.
- [24] Z. Li, L. Liu, S. Dehghan, Y. Q. Chen, and D. Xue, "A review and evaluation of numerical tools for fractional calculus and fractional order controls," *Int. J. Control*, vol. 90, no. 6, pp. 1165–1181, 2017.
- [25] R. Cajo, T. T. Mac, D. Plaza, C. Copot, R. De Keyser, and C. Ionescu, "A survey on fractional order control techniques for unmanned aerial and ground vehicles," *IEEE Access*, vol. 7, pp. 66864–66878, 2019.
- [26] A. Tepljakov, B. B. Alagoz, C. Yeroglu, E. A. Gonzalez, S. H. Hosseinnia, E. Petlenkov, A. Ates, and M. Cech, "Towards industrialization of FOPID controllers: A survey on milestones of fractional-order control and pathways for future developments," *IEEE Access*, vol. 9, pp. 21016–21042, 2021.
- [27] S. Kang, H. Wu, X. Yang, Y. Li, L. Pan, and B. Chen, "Fractional robust adaptive decoupled control for attenuating creep, hysteresis and cross coupling in a parallel piezostage," *Mech. Syst. Signal Process.*, vol. 159, Oct. 2021, Art. no. 107764.
- [28] C. I. Muresan, R. De Keyser, I. R. Birs, S. Folea, and O. Prodan, "An autotuning method for a fractional order PD controller for vibration suppression," in *Mathematical Methods in Engineering (Nonlinear Systems and Complexity)*, vol. 24, K. Taş, D. Baleanu, and J. Machado, Eds. Cham, Switzerland: Springer, 2019, doi: 10.1007/978-3-319-90972-1_15.
- [29] C. Monje, Y. Chen, B. Vinagre, D. Xue, and V. Feliu, *Fractional Order Systems and Control—Fundamentals and Applications*. 2010.
- [30] I. Birs, D. Copot, C. Muresan, R. De Keyser, and C. Ionescu, "Robust fractional order PI control for cardiac output stabilisation," *IFAC-PapersOnLine*, vol. 52, no. 1, pp. 994–999, 2019.
- [31] C. Muresan, C. Copot, I. Birs, R. De Keyser, S. Vanlanduit, and C. Ionescu, "Experimental validation of a novel auto-tuning method for a fractional order PI controller on an UR10 robot," *Algorithms*, vol. 11, no. 7, p. 95, Jun. 2018.
- [32] J. Juchem, C. Muresan, R. De Keyser, and C.-M. Ionescu, "Robust fractional-order auto-tuning for highly-coupled MIMO systems," *Heliyon*, vol. 5, no. 7, Jul. 2019, Art. no. e02154. [Online]. Available: <https://www.sciencedirect.com/science/article/pii/S2405844019358141>
- [33] R. De Keyser, C. I. Muresan, and C. M. Ionescu, "An efficient algorithm for low-order direct discrete-time implementation of fractional order transfer functions," *ISA Trans.*, vol. 74, pp. 229–238, Mar. 2018.



ISABELA BIRS received the Ph.D. degree in fractional order models enabling control strategies based on material properties from Ghent University, Belgium, and the Ph.D. degree in advanced control strategies for poorly damped systems from the Technical University of Cluj-Napoca, Romania. Her research interests include the application of fractional-order calculus to model complex physical phenomena, fractional order control, and cyber-physical systems.



CRISTINA MURESAN received the Ph.D. degree in advanced control of nuclear processes from the Technical University of Cluj-Napoca, Romania, in 2011. She is currently an Associate Professor with the Technical University of Cluj-Napoca. Her research interests include control of various processes, dead-time compensation, and fractional-order control.

MARCIAN MIHAI, photograph and biography not available at the time of publication.



EVA DULF (Senior Member, IEEE) received the Ph.D. degree from the Technical University of Cluj-Napoca, Cluj-Napoca, Romania, in 2006. She is currently a Professor with the Department of Automation, Technical University of Cluj-Napoca. She has published more than 150 papers and received 39 awards at prestigious international exhibitions of inventions. She has been and currently is involved in more than 30 research grants, all dealing with modeling and control of complex processes. Her research interests include modern control strategies, fractional order control, modeling of biochemical, and medical processes.



ROBIN DE KEYSER received the M.Sc. degree in electromechanical engineering and the Ph.D. degree in control engineering from Ghent University, Gent, Belgium, in 1974 and 1980, respectively. He is currently an Emeritus Senior Professor in control engineering with the Faculty of Engineering and Architecture, Ghent University. His research interests include model-predictive control, auto-tuning and adaptive control, modeling and simulation, and system identification.